INT. J. REMOTE SENSING, 10 NOVEMBER, 2004,
VOL. 25, NO. 21, 4629–4639

Taylor & Francis
Taylor & Francis Group

A maximum entropy approach to satellite quantitative precipitation estimation (QPE)

F. J. TAPIADOR*, C. KIDD

School of Geography, Earth and Environmental Sciences, University of Birmingham, Birmingham B15 2TT, UK

V. LEVIZZANI

Institute of Atmospheric Sciences and Climate, National Research Council, I-40129 Bologna, Italy

and F. S. MARZANO

Department of Electric Engineering, University of L'Aquila, I-67040 L'Aquila, Italy

(*Received 11 July 2003; in final form 3 February 2004*)

Abstract. This paper presents a new algorithm to generate quantitative precipitation estimates from infrared (IR) satellite imagery using passive microwave (PMW) data from Special Sensor Microwave/Imager sensor (SSM/I) satellites as ancillary information. To generate the estimates, we model the probabilistic distribution function (PDF) of the rainfall rates through the maximum entropy method (MEM), applying a cumulative histogram matching (HM) technique to the IR brightness temperatures. This results in a straightforward algorithm that can be formulated as an algebraic expression, providing a simple method to derive rainfall estimates using only IR data. The main application of the method is the direct estimation of rainfall rates and accumulated rainfall from geostationary satellites, providing appropriate temporal and spatial resolutions (up to 15 min/4 km when the Meteosat Second Generation satellite becomes available). The proposed method can be easily applied at GOES or current Meteosat satellite reception stations to generate instantaneous rainfall rates estimates with little computational cost. Here we provide examples of applications using the Global Infrared Database and Meteosat images. Our results have been compared with GOES Precipitation Index (GPI) and validated against Global Precipitation Climatology Centre (GPCC)-land rain gauge measurements, at 5°, monthly accumulations. We have obtained correlations of 0.88 for the algorithm, while the GPI yields correlations of 0.85. Preliminary comparisons with other algorithms over Australia also show how the performances of the algorithm are similar to those of more complex models. Finally, we propose some improvements and fine-tuning procedures that can be applied to the algorithm.

*Corresponding author; Present address: Department of Geography, University of Lleida, Spain; e-mail: f.tapiador@geosoc.udl.es, javier@tapiador.com

International Journal of Remote Sensing
ISSN 0143-1161 print/ISSN 1366-5901 online © 2004 Taylor & Francis Ltd
http://www.tandf.co.uk/journals
DOI: 10.1080/01431160410001710000

1. Introduction

The modelling of the rainfall rates has a major importance not only in climatology but also in other fields such as natural hazards assessment or agriculture (Short *et al.* 1989, Kedem *et al.* 1990a, b). While rainfall rates are important by themselves accumulative-derived values can be used to provide rainfall total statistics by multiplying the estimated rainfall rate value by the duration of the rain event.

Rainfall rates can be measured using ground-based devices such as optical rain gauges or impact disdrometers. These measurements have the major drawback of large spatial scattering. Moreover, only a few countries are capable of providing timely and accurate coverage. Because of this, rainfall rates are derived not from these instruments but indirectly from rain gauges. This approach has proved valid to some extent as noted by Sandham *et al.* (1998): if the aim is to provide any kind of global quantitative ground estimation, it is unavoidable to resort to this simplification.

Passive microwave (PMW) sensors aboard satellites are able to provide direct rainfall rates measurements based on the measurement of the natural microwave emission of the Earth. As raindrops affect the upwelling energy at these frequencies, radiation received by the satellite is closely related to the actual rain. This represents an improvement over visible/infrared (VIS/IR) estimations in so far as the cloud top temperature is only indirectly related with cloud-base precipitation.

The Special Sensor Microwave/Imager sensor (SSM/I) aboard the Defense Meteorological Satellite Program (DMSP) satellites uses this physical principle to retrieve rainfall rates for almost global coverage. The quality of these satellite-based estimations has been tested in several intercomparison projects, such as the Algorithm Intercomparison Projects AIP-1, -2 and -3 (Ebert 1996) and the Precipitation Intercomparison Project (PIP-1, -2, -3). PIP-2 was specifically focused on PMW observations (Smith *et al.* 1998) while AIP-3 (Adler *et al.* 2001) also generated some results on PMW proving the better capabilities in instantaneous rainfall retrieval of the PMW compared with IR/VIS estimates. Therefore, it can be stated that more consistent global rainfall measurements are available for instantaneous rainfall estimates from the PMW sensors, such as the SSM/I.

Several attempts have been made to find a mathematical probability distribution function (PDF) that matches the frequency of rain-rate occurrence. Wilheit *et al.* (1991) and Kedem *et al.* (1990a) used gamma and lognormal distributions obtaining encouraging results. In particular, Kedem *et al.* (1994) present an axiomatically based lognormal and mixed lognormal probability distribution model instead of an empirical approach. Here, we have taken another approach using a new theoretically derived sub-exponential distribution, which provides a fit for tropical rainfall rates of $\sim 0.98\ R^2$ when compared with the observed SSM/I estimates. The aim of this paper is to show how these results can be applied to generate global rainfall estimates using Meteosat IR and the Global IR database satellite data (Janowiak *et al.* 2001). This differs from other approaches such as GPI or the Autoestimator (Vicente *et al.* 1998) that are based on empirical fits with rainfall measurements.

2. Data sources

2.1. *SSM/I data*

The DMSP carries the enhanced SSM/I system, the first or which (F8) was launched in 1987. The latest SSM/I (F15) was launched in December 1999, becoming operational in February 2000. The SSM/I sensor measures the Earth's microwave emission and has a near-circular, Sun-synchronous, near-polar orbit at an altitude of 860 km with an inclination of 98.8° and an orbital period of 102 min.

This provides complete coverage of the Earth, excluding two 2.4° circular sectors centred on the poles. Spatial sampling resolution is 12.5 km at 85 GHz and 25 km at the lower frequencies. Calibration is done once each satellite rotation (period 1.899 s) with a cold (3.1 K) and a warm (300 K) target. This ensures that the measured signal has a good precision.

SSM/I data were obtained through the Global Hydrology Resource Center at NASA's Marshall Space Flight Center. More than 70 GB of SSM/I overpasses (14 months of images) were processed to obtain the rainfall estimates for validation. Many rainfall-rate retrieval algorithms have been proposed (Ferraro 1997, Smith *et al*. 1998). Here, a frequency difference algorithm is used: the physical basis is that the 85 GHz channel will be more affected than the lower 19 GHz frequency by the scattering from precipitation-sized particles. Rain rates (RR) are generated through a look-up table derived from coincident measurements with TRMM Precipitation Radar (PR) data, and the aim is to minimize the effects of surface temperature, emissivity and atmospheric effects. Vertical channels are used over the ocean, with the horizontal polarization used over land areas. Estimates over coastal regions are produced by a polarization-corrected temperature algorithm (Kidd 1998).

2.2. *Global IR database data*

Since the VIS images cannot be used during night-time only the IR is considered to provide a complete daily series of rainfall estimates. Globally merged, full-resolution ($\sim$4 km), radiometrically corrected IR data from the Climate Prediction Center are used as the source of IR information. These Global IR data are generated from the $\sim$11 μm IR channels on board the GMS-5, GOES-8, GOES-10, Meteosat-7 and Meteosat-5 geostationary satellites and are resampled to 0.036° resolution. Details are provided by Janowiak *et al*. (2001).

2.3. *Meteosat data*

Meteosat images have also been used to show the capabilities of the algorithm in an operative framework. Providing a straightforward method to generate rainfall rates inside the processing flow was considered an important issue in terms of the practical application of the method, since many users routinely receive these images. We have used both Meteosat A and B formats: Meteosat A format data corresponding with several Intensive Observation Programs (IOPs) of the Mesoscale Alpine Project (MAP) have been used to generate the rainfall rates from our algorithm. These data have been provided by the EUMETSAT archive service. Meteosat B format images received in real time from a satellite reception station have also been used to prove the operational capabilities of the algorithm.

3. Methods

3.1. *Maximum entropy modelling*

We have modelled the PDF of the rainfall rates based upon the maximum entropy method (MEM). The MEM (Jaynes 1963, 1990) states that the most likely PDF based on the information available is given by maximizing the entropy function subject to the constraints of the system. In the rainfall intensity problem

we have assumed the following constraints:

$$\int_k^\infty p(x_i)\mathrm{d}x = 1 \tag{1}$$

$$\int_k^\infty \log\left(\frac{x_i - a}{b}\right) p(x_i)\mathrm{d}x = E\left[\log\left(\frac{x_i - a}{b}\right)\right] \tag{2}$$

$$\int_k^\infty \log\left[\left(1 + \frac{x_i - a}{b}\right)^{-c}\right] p(x_i)\mathrm{d}x = E\left[\log\left(1 + \frac{x_i - a}{b}\right)^{-c}\right] \tag{3}$$

Where $p(x)$ is the PDF of the rainfall rates x; a, b and c are the parameters of the distribution; and E is the expectation. These three assumptions are based on the observation of the rainfall rates PDFs. Equation (1) is the normalization condition, equation (2) is a random walk on the logarithmic scale, and equation (3) is a random walk in the logarithmic scale of the accumulated PDF. Maximizing the entropy function S:

$$S \equiv -\int_k^\infty p(x_i)\log p(x_i) \tag{4}$$

subject to (equations (1), (2), (3)) the application of the MEM yields:

$$p(x) = \frac{a \cdot c}{b}\left(\frac{x - a}{b}\right)^{-c-1}\left[1 + \left(\frac{x - a}{b}\right)^{-c}\right]^{-d-1} \tag{5}$$

When fewer than four constraints are used, it is possible to solve the MEM analytically following the ingenious procedure proposed by Singh *et al.* (1986). If more constraints are required to model the process, numerical methods must be used, but the problem always has a solution.

Our work shows that equation (5) matches tropical rainfall rates derived from SSM/I with a high degree of accuracy: by taking a whole year of SSM/I tropical overpasses, parameterizing the PDF (see §3.3) and then comparing the actual SSM/I histogram with the PDF derived by equation (5), we have obtained significant matches as can be seen in figure 1. These results are interesting by themselves since they show a parameterization of the rainfall rates based upon different hypotheses than those yielding gamma and lognormal distributions. But in terms of the rainfall rate estimate, this PDF can be used to improve the temporal resolution of the estimates by combining it with IR cloud top temperatures through a histogram matching (HM) technique. It is worth noting here that we presume that, as in the classical HM techniques, SSM/I observations are the best available measure of rainfall rates at the global scale and then considered as the reference rainfall. Nonetheless, the method presented here can be applied to any other rainfall measurement.

The procedure we describe here takes advantage of the fact that if equation (5) represents a good fit with measurements within the narrow SSM/I swathe, we need only the moments of the PDF, instead of the whole empirical histogram, to derive rainfall rates for the areas near but outside the swathe. More importantly, the

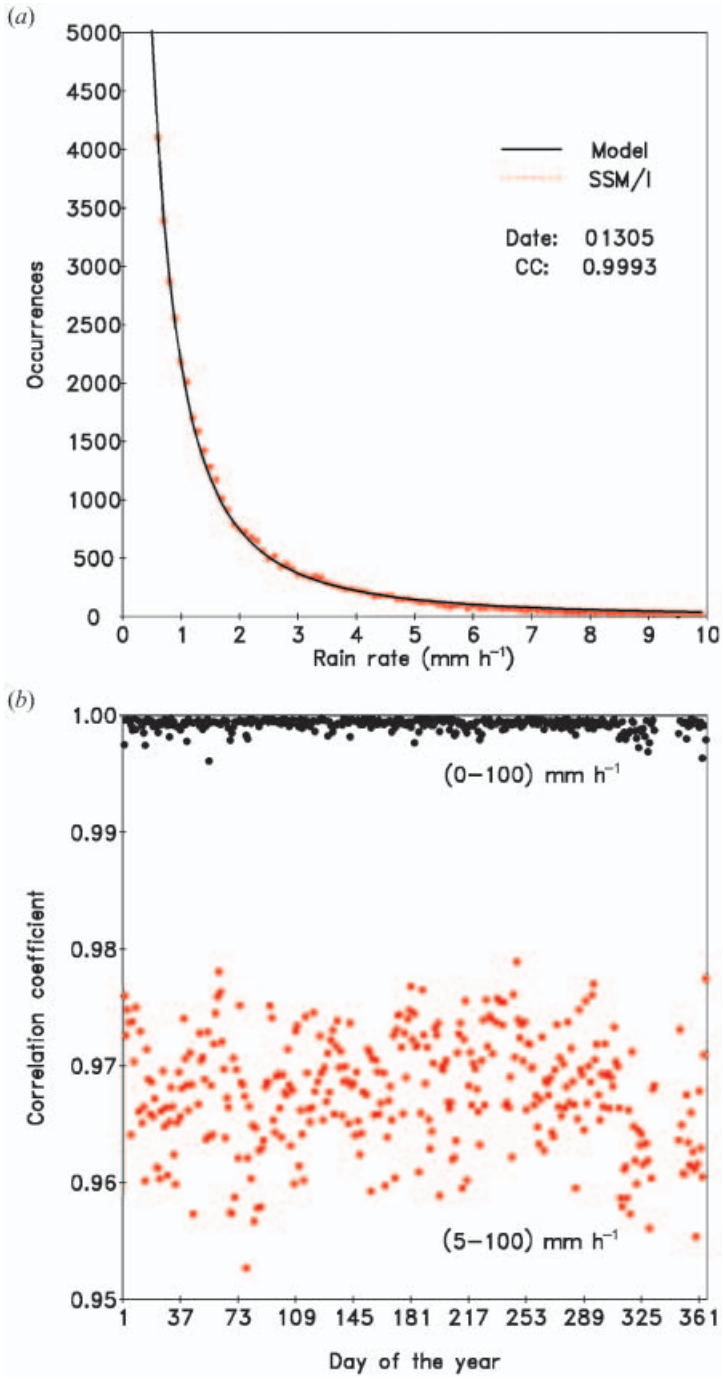

Figure 1. Fit of the model with a daily sample observation (*a*) and correlations obtained for the year 2001 for tropical rainfall (*b*), including conditional and unconditional correlations.

mean, the standard deviation and the mode of the rainfall rates can be considered as macrostate variables that we can assume are independent of the scale of the observation. These three moments give us information about the probability of

each rain rate, considered here as a microstate. Although this microstate can only be inferred, the macrostate variables are extensive quantities that can be easily measured. If we now suppose that SSM/I represents the truth, we can parametrize equation (5) to obtain the PDF. The last step is to consider as rainy pixels those below a threshold (for instance 235 K as the GPI does) in the IR image, and assign to them the rainfall rates using a cumulative HM technique.

3.2. *The histogram matching method*

Many cumulative HM methods have been proposed to blend passive microwave data with those provided by the geostationary IR sensors such as GOES or Meteosat. The advantages of this procedure have been discussed in depth in many papers. We follow here the method proposed by Crosson *et al.* (1996), which establishes a relationship between the probability PDF of the PMW rain rate x and the IR brightness temperatures T.

$$\int_{R_i}^{R_j} p(x)\mathrm{d}x = \int_{T_i}^{T_j} p(T)\mathrm{d}T \tag{6}$$

The PMW rain rate PDF is matched by accumulating the IR starting from the warm end and generating a series of matched pairs; that is, satisfying the following expression (Turk *et al.* 1998):

$$\frac{\int_{R_i}^{R_j} x^m p(x)\mathrm{d}x}{\int_{R_i}^{\infty} x^m p(x)\mathrm{d}x} = \frac{\int_{T_i}^{T_j} T^m p(T)\mathrm{d}T}{\int_{T_i}^{\infty} T^m p(T)\mathrm{d}T} \tag{7}$$

where m is the moment order. After processing the (T,r) pairs as described, the time update cycle writes out a file that contains a lookup table for each selected box that relates the IR temperature to the PMW rain rate, including the zero-rain-rate IR temperature threshold. This file can then be used to match the histograms of subsequent images, providing a complete series of rainfall rate estimates at the temporal resolution of the IR. Notice that we apply the histogram matching not to the PMW data itself but to the MEM modelled PDF. Thus, this theoretical PDF depends on four parameters that can be related with the radiances measured with SSM/I.

The method is visualized in figure 2. The SSM/I near-polar orbit can provide more precise instantaneous rainfall estimates than IR-based satellites, but for a narrow swathe and with a limited time resolution. However, it may be considered as a statistically representative set (a sample) of a larger area. Using this sample, the moments of the modelled PDF can be estimated, providing a consistent histogram for the whole area, not only for the swathe. Notice that the use of the histogram outside swathe limits cannot be properly justified since we cannot guarantee that the histogram would be exactly the same. The MEM is used to calculate the most likely histogram of the (unlimited) number that could happen, using only the information available. The MEM gives the least biased estimate amongst all the possible histograms, so in this sense the method is optimum. This represents a difference over simple curve-fitting to a given function such as the gamma or the lognormal, in so far that we have calculated the most suitable PDF from a set of

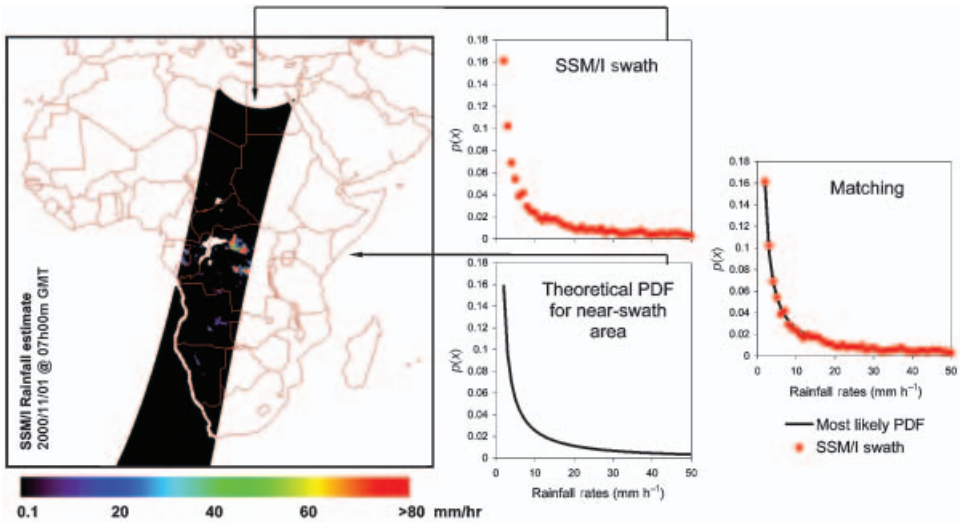

Figure 2. An example illustrating the logic of the algorithm. The histogram of the rainfall rates (named *SSM/I swath*) is a statistical sample of the neighbourhood that allows us to calculate some moments. By applying the maximum entropy method, we can establish the most likely PDF for the whole population. Thus, the curve named *theoretical PDF for near-swath area* represents a PDF valid not only for the SSM/I swath but for the neighbourhood. Comparing this PDF with the actual histogram for the SSM/I swath (*matching* graph), the differences are negligible: the use of the histogram matching technique either with the actual histogram or with the maximum entropy PDF makes little or no difference for the swath estimates, but gives us additional estimates outside it.

simple hypotheses, and we can be certain that this is the PDF derived from all the information we have.

3.3. *Parameter estimation*

Once the PDF has been theoretically estimated using the MEM, the SSM/I data are used for parameter estimation. Once the PDF is known, the moments of the distribution can be calculated using the MEM as demonstrated by Singh *et al.* (1986) with the added advantage that the moments appear naturally from the constraints from the population expectations instead of from sample averages. The method of moments (MOM), maximum likelihood estimation (MLE) or probability-weighted moments (PWM) can also be used. Solving:

$$\mu = a + \frac{b\Gamma\left(1-\frac{1}{c}\right)\Gamma\left(\frac{1}{c}+d\right)}{\Gamma(d)} \tag{8}$$

$$\sigma^2 = \frac{kb^2}{\Gamma^2(d)} \tag{9}$$

$$\text{mode} = a + b\left(\frac{cd-1}{c+1}\right)^{1/c} \Leftrightarrow cd > 1, \text{ else mode} = a \tag{10}$$

$$median = a + b\left(2^{1/d}-1\right)^{-1/c} \tag{11}$$

where $\Gamma(x)$ is the gamma function: $\Gamma(x) \equiv \int_0^\infty t^{x-1}\exp(-t)\mathrm{d}t$, μ is the mean and σ is

the variance of the distribution. Solving equations (8)–(11) using a recursive algorithm provides the parameters a, b, c, d for the equation (5) and gives the PDF. This parametrization can be done either in real time, using the last available SSM/I data, or using any amount of rainfall-rate data history. Preliminary tests (not shown here) have revealed that the parameters are geographically related and can even be used to characterize the rainfall climatology of a given area.

4. Results

The resulting PDF (equation (5)) fits rainfall rates with a high correlation: using a year of SSM/I tropical swathes we have calculated the PDF with the SSM/I estimates and then we compared them with the MEM predictions. Figure 1 shows the correlations obtained for conditional (not including zero rain) and unconditional (including zero rain) rainfall. As can be seen, the fit is very good. The PDFs vary slightly from day to day, but it is noticeable how steady they are. Randomly selecting one parametrization and applying it to the rest of the estimates, the results are still above 0.90 R^2 for conditional rainfall rates. Typical values of the parameters are $a \in (0.1,1.0)$, $b \in (0.1,0.5)$, $c \in (0.6,1.5)$ and $d \in (1.0,8.0)$. While it is clear that the parameterization varies regionally further analysis will be required to find out if these variations reflect any climatological or meteorological process. These parameters might be used to characterize different rainfall regimes, since it is well known that the PDF for frontal, orographic and convective rainfall differ. It is also noticeable that the proposed PDF adapts well to different situations using different parameters: the only requirement is to have a representative set. Also, if the method is to be applied to other than a large scale, other parametrizations could be required. The parameters can be calculated using equations (8)–(11).

Figure 3 shows the application of the algorithm to a Meteosat format A IR image. The main rainfall patterns at geostationary scale are clearly visible, providing 4 km/30 min rainfall estimates. Using the same procedure presented here

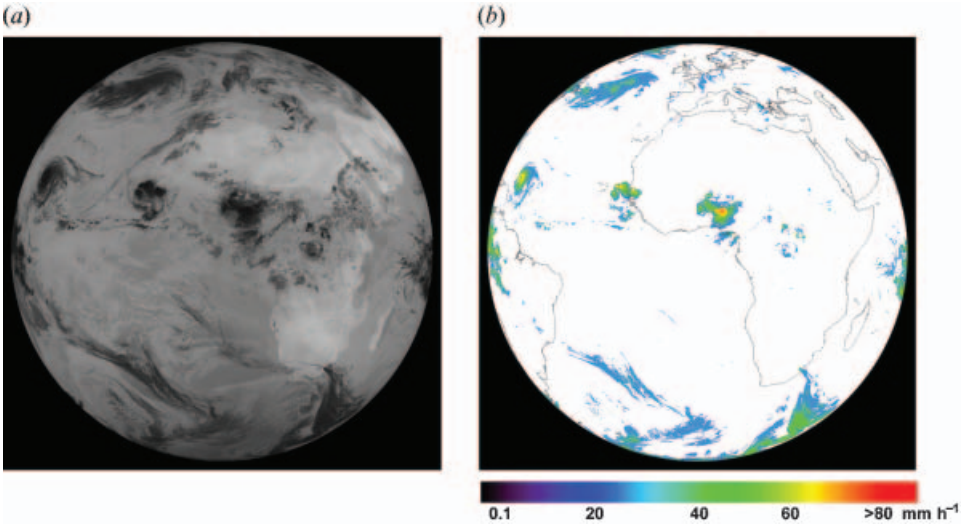

Figure 3. Meteosat format A High Resolution (HR) image (*a*) and the rainfall estimate (*b*) provided by the algorithm.

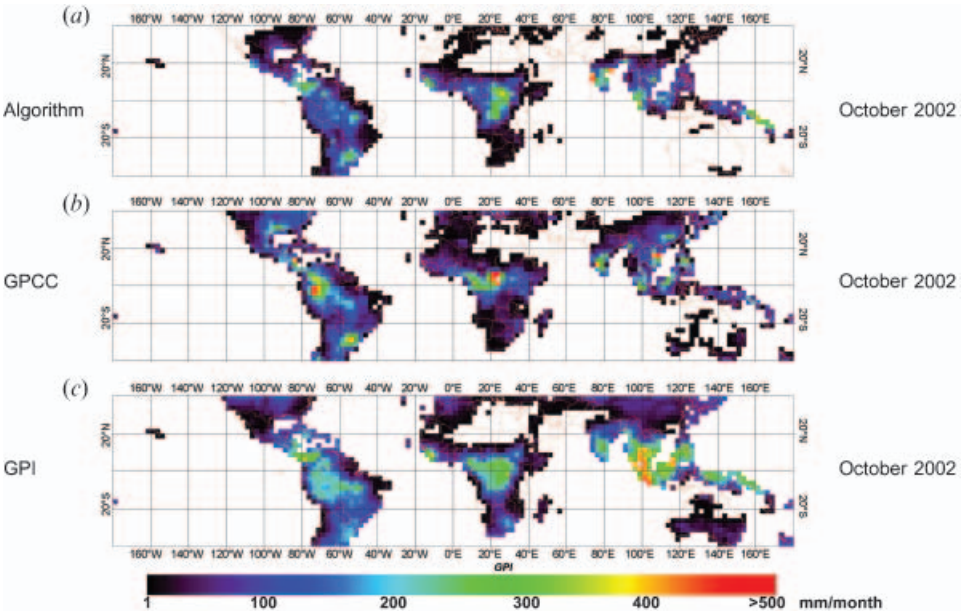

Figure 4. Comparison for the E/A algorithm (*a*), GPCC gauge data (*b*) and GPI (*c*) for monthly-accumulated (October 2002) estimates at 2.5° resolution.

with data from the new Meteosat Second Generation satellite, 15 min estimates can be obtained (see Levizzani *et al.* 2001).

Figure 4 shows routine global estimates combining most of the geostationary satellites in the Global IR database (Janowiak *et al.* 2001). The original resolution of the IR information is 4 km. Validation against gauge-GPCC monthly estimates shows correlations above 0.75 R^2 for $2.5^\circ \times 2.5^\circ$ estimates and ~ 0.88 for $5.0^\circ \times 5.0^\circ$ (figure 5).

Figure 5 also shows a comparison between the algorithm and the GPI. As can be seen, the algorithm slightly improves the overall GPI performances. The algorithm is clearly superior in Australasia (0.92 R^2 vs 0.87 R^2 when compared against gauges), but shows little improvement over the Americas (0.80 vs 0.78) and over Africa (0.73 vs 0.70). Comparison against a dense net of rain gauges is currently being carried out over Australia following the tools in satellite rainfall validation (Ebert 2002a, b). Preliminary results show that the algorithm is comparable in performance to other approaches. A complete picture of the validation strategy and results can be obtained at: http://www.bom.gov.au/bmrc/wefor/staff/eee/SatRainVal/sat_val_aus.html.

Documentation and sample programs for applying the algorithm to Meteosat A and B format images can be found in the *World Meteorological Organisation's International Precipitation Working Group* web pages under the name of *EURAINSAT/A algorithm* (http://www.isac.cnr.it/~ipwg/algorithms.html).

5. Conclusions

A new straightforward algorithm to derive rainfall rates from IR satellite images has been presented. The method uses a simple function to derive the theoretical PDF of the rainfall rates at a global scale, and uses the histogram matching technique to assign these rainfall rates to the *a priori* raining IR pixels. The

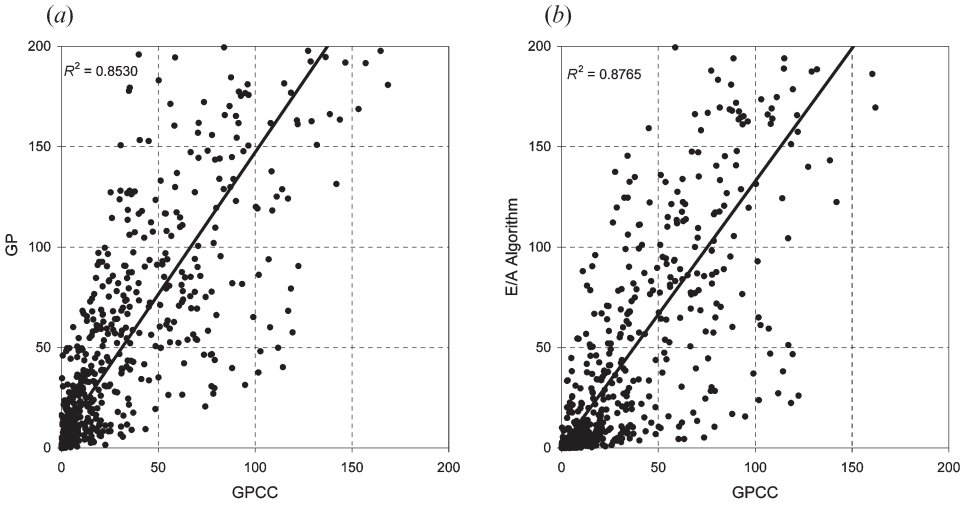

Figure 5. Scatter plots for October 2002 estimates between 40° N and 40° S latitude at 5° resolution: (*a*) comparison between GPI estimates and GPCC-land gauges measurements; and (*b*) comparison of the algorithm against the same gauge data. The straight line is the linear regression.

rationale behind the procedure is the use of the maximum entropy method (MEM) to establish the PDF of the global rainfall rates. This PDF has been validated against SSM/I measurements having correlations around 0.99 R^2 for unconditional estimates, and is used here to generate the rainfall estimates using the cumulative histogram matching (CHM) technique. Compared with other more complicated methods such as Neural Networks, the algorithm presented here also has the major advantage of its simplicity and easy implementation. Finally, validation against GPCC gauge data shows a reasonable correlation against gauge estimates.

Acknowledgments

This research was funded by the EURAINSAT project, a shared-cost project (contract EVG1-2000-00030), co-funded by the Research DG of the European Commission within the RTD Activities of a Generic Nature of the Environment and Sustainable Development sub-programme (5th Framework Programme). Also acknowledged are the EUMETSAT archive service for providing the METEOSAT *format A* images; the Climate Prediction Center/NCEP/NWS and John Janowiak for the Global IR database; and the Global Hydrology Resource Center, NASA's Marshall Space Flight Center for the SSM/I data.

References

ADLER, R. F., KIDD, C., PETTY, G., MORISSEY, M., and GOODMAN, H. M., 2001, Intercomparison of global precipitation products: the Third Precipitation Intercomparison Project (PIP-3). *Bulletin of the American Meteorological Society*, **82**, 1377–1396.

CROSSON, W. L., DUCHON, C. E., RAGHAVAN, R., and GOODMAN, S. J., 1996, Assessment of rainfall estimates using a standard Z–R relationship and the probability matching method applied to composite radar data in central Florida. *Journal of Applied Meteorology*, **35**, 1203–1219.

EBERT, E. E., 1996, Results of the 3rd Algorithm Intercomparison Project (AIP-3) of the

Global Precipitation Climatology Project (GPCP), Revision 1. Bureau of Meteorology Research Centre, Melbourne, Australia.

EBERT, E. E., 2002a, Verifying satellite precipitation estimates for weather and hydrological applications. *1st International Precipitation Working Group (IPWG) Workshop, Madrid, Spain, 23–27 September 2002*.

EBERT, E. E., 2002b, Verification of precipitation forecast. *International Conference on Quantitative Precipitation Forecasting, Reading, UK, September 2002*.

FERRARO, R. R., 1997, SSM/I derived global rainfall estimates for climatological applications. *Journal of Geophysical Research*, **102**, 16 715–16 735.

JANOWIAK, J. E., JOYCE, R. J., and YAROSH, Y., 2001, A real-time global half-hourly pixel-resolution infrared dataset and its applications. *Bulletin of the American Meteorological Society*, **82**, 205–217.

JAYNES, E. T., 1963, Information theory and statistical mechanics. In *Statistical Physics*, edited by K. Ford (New York: Benjamin).

JAYNES, E. T., 1990, Probability theory as logic. In *Maximum-Entropy and Bayesian Methods*, edited by P. F. Fougère (Dordrecht, The Netherlands: Kluwer).

KEDEM, B., CHIU, L. S., and KARNI, Z., 1990, An analysis of the threshold method for measuring area average rainfall. *Journal of Applied Meteorology*, **29**, 3–20.

KEDEM, B., CHIU, L. S., and NORTH, G. R., 1990, Estimation of the mean rain rate: application to satellite observations. *Journal of Geophysical Research*, **95**, 1965–1972.

KEDEM, B., PAVLOPOULOS, H., GUAN, X., and SHORT, D. A., 1994, A probability distribution model for rain rate. *Journal of Applied Meteorology*, **33**, 1486–1493.

KIDD, C., 1998, On rainfall retrieval using polarization-corrected temperatures. *International Journal of Remote Sensing*, **19**, 981–996.

LEVIZZANI, V., SCHMETZ, J., LUTZ, H. J., KERKMANN, J., ALBERONI, P. P., and CERVINO, M., 2001, Precipitation estimations from geostationary orbit and prospects for Meteosat Second Generation. *Meteorological Applications*, **8**, 23–41.

SANDHAM, L. A., SEED, A. W., and VAN RENSBURG, P. A. J., 1998, The relationship between half-hourly rainfall occurrence and daily rainfall. *Water South Africa*, **24**, 101–106.

SHORT, D. A., WOLFF, D. B., ROSENFELD, D., and ATLAS, D., 1989, A rain-gauge, radar and satellite simulation study of the estimation of convective rainfall by area–time integrals. *Proceedings of the Fourth Conference on Satellite Meteorology and Oceanography, San Diego, CA* (Boston, MA: American Meteorological Society), pp. 90–93.

SINGH, V. P., RAJAGOPAL, A. K., and SINGH, K., 1986, Derivation of some frequency distributions using the principle of maximum entropy (POME). *Advances in Water Resources*, **9**, 91–106.

SMITH, E. A., LAMM, J. E., ADLER, R., ALISHOUSE, J., AONASHI, K., BARRETT, E. C., BAUER, P., BERG, W., CHANG, A., FERRARO, R., FERRIDAY, J., GOODMAN, S., GRODY, N., KIDD, C., KNIVETON, D., KUMMEROW, C., LIU, G., MOZANO, F., MUGNAI, A., OLSON, W., PETTY, G., SHIBATO, A., SPENCER, R., WENTZ, F., WILHEIT, T., and ZIPSER, E., 1998, Results of the WetNet PIP-2 Project. *Journal of Atmospheric Sciences*, **55**, 1483–1536.

TURK, F. J., MARZANO, F. S., SMITH, E. A., and MUGNAI, A., 1998, Using coincident SSM/I and infrared geostationary satellite data for rapid updates of rainfall. *Geoscience and Remote Sensing Symposium Proceedings, IGARSS'98. IEEE International*, **1**, 150–152.

VICENTE, G., SCOFIELD, R. A., and MENZEL, W. P., 1998, The operational GOES infrared rainfall estimation technique. *Bulletin of the American Meteorological Society*, **79**, 1883–1898.

WILHEIT, T. T., CHANG, A. T. C., and CHIU, L. S., 1991, Retrieval of monthly rainfall indices from microwave radiometric measurements using probabilistic distribution functions. *Journal of Atmospheric and Oceanic Technology*, **8**, 118–136.